Central European Journal of Energetic Materials
ISSN 1733-7178; e-ISSN 2353-1843

Cent. Eur. J. Energ. Mater. 2023, *20*(3): 241-259; DOI 10.22211/cejem/172909
Article is available in PDF-format, in colour, at:
https://ipo.lukasiewicz.gov.pl/wydawnictwa/cejem-woluminy/vol-20-nr-3/

Research paper

Experimental Study and Numerical Simulation of Explosive Welding of Nickel Foil with Q235 Steel

Mengben Xu, **Xinghua Xie**[*)], **Hanxin Wang**, **Maaolin Zhu**
School of Chemical Engineering, Anhui University of Science and Technology, Anhui, China
* *E-mail:* xxh1963@163.com

Abstract: In order to study the interface microstructure and formation mechanism of nickel (Ni) foil/steel Q235 (Ni/Q235) explosive composite plate, Ni/Q235 laminated composite was successfully prepared by explosive welding technology using Ni foil, Q235 steel plate as substrate and composite plate. respectively. The microstructure of the bonding interface was analyzed by SEM and EDS. The mechanical properties of the interface were tested by tensile tests. The explosive welding process was simulated by the smooth particle fluid dynamics (Smoothed Particle Hydrodynamics, SPH) numerical simulation method. The results showed that the interface of the Ni/Q235 explosive composite plate had regular wave-like bonding, and there were no defects, such as unbonding and local melting at the bonding interface. The tensile strength of the tensile specimen reached 623 MPa, and the Ni layer and the Q235 layer on either side of the tensile specimen fracture exhibited a mainly plastic fracture. The numerical simulation results were in good agreement with the experimental results, which can provide theoretical support for the study of the explosive welding preparation of Ni/Q235 double-layer composite plate and the bonding mechanism of its connection interface.

Keywords: explosive welding, nickel foil, SPH simulation, mechanism of connection

1 Introduction

Explosive welding, as a special welding technique, uses the huge energy generated by an explosive to drive a high-speed collision between the compound plate and the substrate to form a metallurgical bond between the two [1]. Compared to other welding techniques, the distinguishing feature of explosive welding is the ability to achieve excellent welding results for many materials with vastly different physical properties [2, 3]. Explosive welding has been widely used in the aerospace, automotive, and energy industries, among others, due to its ability to produce metal composites that meet a variety of application environments and reduce manufacturing costs [4, 5].

Q235 steel is characterized by high strength, hardness, and wear resistance, while Ni and Ni alloys have excellent corrosion resistance and process properties, good physical properties, and have special memory and electromagnetism and other functional properties. Ni and Ni alloys have good corrosion resistance in acidic and alkaline conditions, and are also widely used in plate heat exchangers, alkali production and petrochemicals, due to their easy cold working. In nuclear reactor engineering, high Ni alloys such as Inconel 600 are often used to replace 1Cr18Ni9Ti stainless steel in heat exchangers and other equipment in order to avoid stress corrosion. Because metal composites can combine the respective advantages of two metals to complement any shortcomings, greatly improving the performance of a single material, Ni-plated steel has a wide range of application prospects in high-performance battery tanks, corrosion-resistant chemical containers and other fields. However, because Ni is an important non-ferrous metal, its relatively expensive price limits its use to a certain extent. As a functional coating material, economy and efficiency are two important factors in evaluating its application prospects. Current techniques such as chemical Ni plating [6], Ni electroplating [7], *etc.,* are attempts to obtain Ni-plated materials. However, these prepared coatings have disadvantages, such as poor brightness, have corrosion points and uneven thickness. Achieving high melting point and high-quality metal coatings has traditionally been a challenging task. However, explosive welding of metal foils (EWMF) offers a solution to this and can be viewed as a special coating process. It is driven by the energy from the explosion of an explosive charge, through the high-speed parallel impact of the plasma that is formed within several atomic layers of two metal surfaces, so that interatomic bonding is established between the metal surfaces on both sides, resulting in a coating. At the local high temperature and pressure, metallurgical bonding can be achieved by suppressing the generation of a large-scale melt zone due to the transient nature of melting, which occurs at the metal bonding surfaces, followed by rapid cooling [8]. EWMF has gained widespread attention due to its successful applications, such as amorphous foil/Fe [9], $\text{tungsten}_{(\text{foil})}$/Cu [10], metallic $\text{glass}_{(\text{foil})}$/Al [11], and $\text{tantalum}_{(\text{foil})}$/Fe [12], demonstrating its potential for welding a variety of materials.

In the numerical simulation method, this paper has resorted to ANSYS/AUTODYN software and the Smooth Particle Hydrodynamics (SPH) method to simulate the process of $\text{Ni}_{(\text{foil})}/\text{steel}_{(\text{Q235})}$ explosive welding. Extensive research has demonstrated that the SPH method is highly effective for simulating large deformations and gradients, such as those found in explosive welding. For the numerical simulation model, the Mie-Grüneisen equation of state was selected due to its ability to accurately characterize the plastic deformation behaviour of materials under large deformation conditions. To model the kinetic behaviour of the materials during large deformations, the Steinberg-Guinan strength model was selected, based on its effectiveness in describing such behaviour [13].

2 Materials and Methods

2.1 Test materials

The size of the Ni foil (100×160×0.5 mm) as the composite plate was selected in order to avoid boundary effects; the length and width of the Ni foil used were larger than the substrate. The Q235 steel substrate size was 100×150×15 mm. The polyvinyl chloride (PVC) plate size was 100×160×3 mm. The chemical composition and mass fraction of the base plate and composite material are shown in Table 1.

Table 1. Chemical composition (in wt.%) of Ni foil and Q235 steel

Material	Ni	C	Si	S	P	Cu	Mn	Fe	Mg
Ni foil	Bal.	≤0.01	≤0.03	≤0.001	–	≤0.015	≤0.002	≤0.04	≤0.01
Q235	–	≤0.22	≤0.30	≤0.05	≤0.45	–	≤0.55	Bal.	–

An emulsion matrix was selected as the matrix, with hollow glass microspheres as a sensitizer and diluent, the preparation of microsphere content of 20% of low explosive, explosive density of 0.9 g/cm^3, explosive detonation velocity of 2500 m/s. The composition of the emulsion matrix was:

– NH_4NO_3: 71.0 wt.%,
– $NaNO_3$: 11.5 wt.%,
– H_2O: 11.0 wt.%,
– $C_{18}H_{38}$: 3.7 wt.%,

– $C_{24}H_{44}O_6$: 2.8 wt.%.

To ensure uniform explosive density and improve explosive utilization [14], aluminum honeycomb plates were used as explosive frames, and the mixed emulsified explosive was filled into the holes of the honeycomb plates, to prepare a 12 mm thick honeycomb structure charge and placed on top of the welding assembly. In addition, the detonator was positioned in the middle of the short side of the explosive. Due to the fragility of the metal foil during the explosive welding process, high speed collisions can produce defects such as wrinkles, cracks and voids in the metal foil. In order to protect the Ni foil from ablation and reduce impact damage [16], a buffer structure consisting of a 1 mm thick copper plate and a 3 mm thick PVC plate was placed on the upper surface of the Ni foil.

2.2 Test methods

In this work, the parallel placement method was used for the explosive welding test, with the selection of a low explosive velocity emulsion explosive for welding. The stand-off distance between the base and flyer layers was 3 mm. Before the welding test, the inner surface of the plate was polished clean with sandpaper and cleaned with anhydrous ethanol. The explosive welding assembly was then placed on the table in a spherical tank. The explosive welding structure diagram is shown in Figure 1. After the explosive welding process, metallographic samples of the Ni/Q235 composite were cut along the direction of the blast wave propagation using a wire cutter. The samples were then ground and polished, and the waveform morphology of the bonding interface was observed using a scanning electron microscope (SEM) (Talos F200i). Energy-dispersive X-ray spectroscopy (EDS) was used to determine the distribution and composition of elements at the bonding interface. Finally, an electronic universal testing machine (GNT600) was used to characterize the mechanical properties of the weld; the dimensions of the tensile specimen are shown in Figure 2.

Figure 1. Explosive welding structure diagram

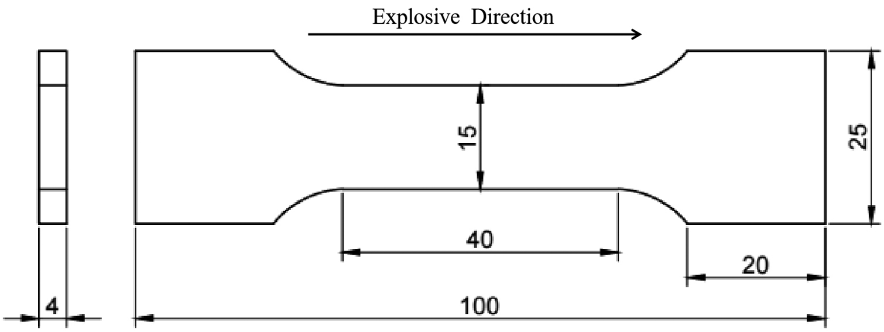

Figure 2. Schematic diagram of a tensile specimen (dimensions in mm)

3 Test Results and Analysis

3.1 Analysis of the interface waveform characteristics

With the test parameters used in this work, a Ni/Q235 composite plate was prepared and the microstructure at the bonding interface was observed using scanning electron microscopy. As shown in Figure 3, the Ni/Q235 bonding interface exhibits a regular wavy shape, without any unbonded areas or local melting defects. This wavy interface is an important indicator of high-quality welding, as it significantly increases the bonding area and forms an interlocking effect, effectively improving the interface bond strength [17]. During the explosive welding process, the nickel foil collides with the Q235 steel at high speed, and the mechanical energy released during the collision leads to a rapid pressurization of the two materials and a strong plastic flow in the interfacial region. Nickel metal particles are involved in the vortex during the movement and eventually form a molten block covered by the substrate, as shown in Figure 4. This is in agreement with the phenomenon observed previously [18].

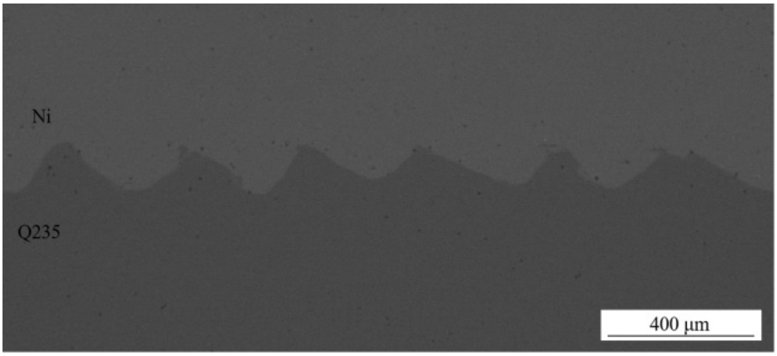

Figure 3. Waveform morphology of Ni/Q235 welded composite plate bonding interface

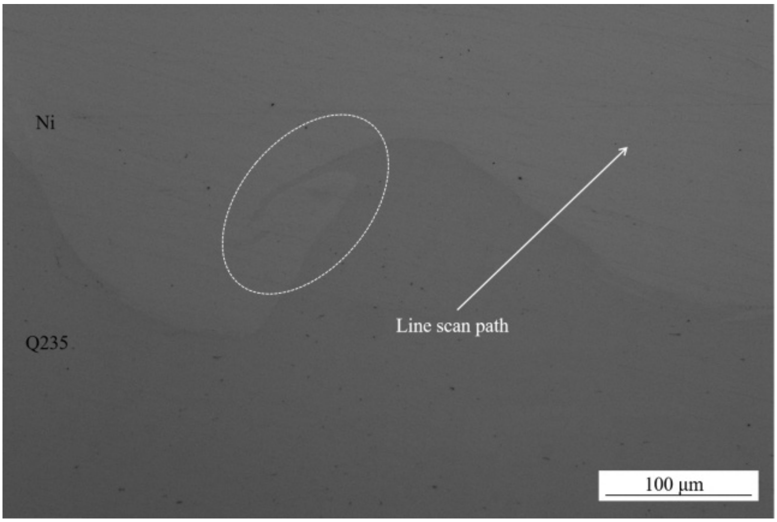

Figure 4. Melting zone at line scan path and crest

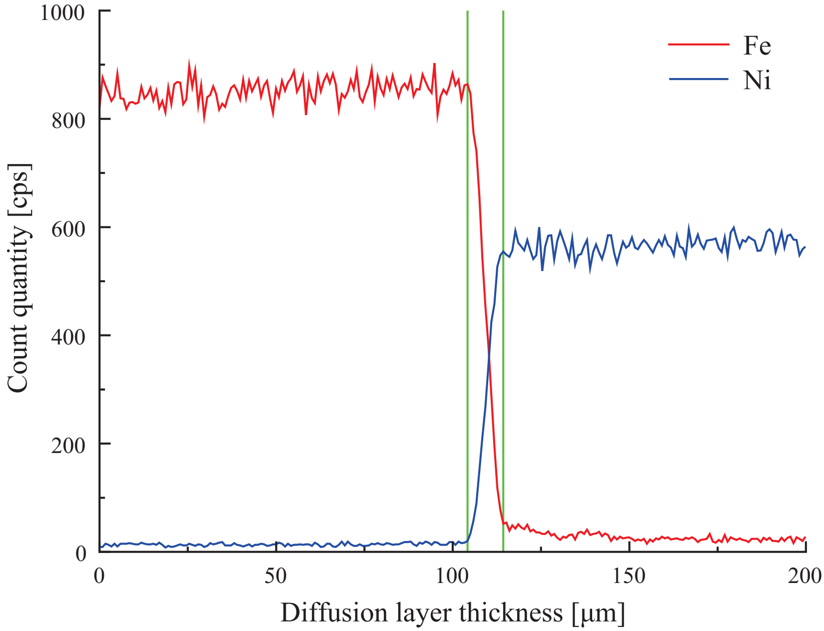

Figure 5. Line scan results at the Ni/Q235 interface

The laminate has undergone an elemental transformation from Fe to Ni at the Ni/Q235 interface, which is very likely to produce brittle intermetallic compounds during the interfacial atomic diffusion process. Therefore, in addition to the analysis of the interface microscopic morphology, it is also important to check the interfacial bonding quality for the possibility of brittle intermetallic compounds. Further analysis of the bonding interface using EDS line scan (Figure 5) shows that a significant diffusion phenomenon occurs at the Ni/Q235 bonding interface, and the thickness of the diffusion layer can be seen to be about 10 μm, from the two vertical thin lines dividing the range in Figure 5. The line scan curve did not have a significant step phenomenon, so the diffusion did not produce brittle intermetallic compounds.

3.2 Analysis of the mechanical properties

To verify improvement in the welding quality of the composite plate, tensile strength testing was conducted using a universal testing machine, as shown in Figure 6. Tensile testing was performed with reference to the national standard GB/T228-200 [19]. The tensile strength of substrate Q235 steel and Ni were 400 and 380 MPa, respectively. The Ni/Q235 composite plate exhibited a tensile strength of approximately 623 MPa, which is higher than the theoretical value calculated using Equation 1 and meets the requirements for product use.

$$R_m = \frac{R_1 d_1 + R_2 d_2}{d_1 + d_2} \tag{1}$$

where R_m is the tensile strength of the composite plate (in MPa), R_1, R_2 are the tensile strengths of the composite plate and of the substrate (in MPa) respectively, and d_1 and d_2 are the thicknesses of the composite plate and of the substrate (in mm) respectively. Introducing these values into Equation 1, the theoretical value of the tensile strength of the Ni/Q235 composite plate should be 397.5 MPa.

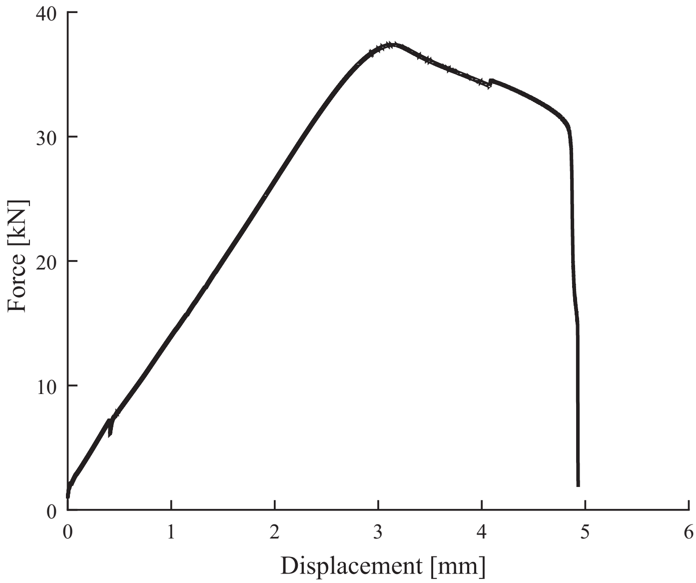

Figure 6. Tensile curve of Ni/Q235

Figure 7 shows the appearance of the Ni/Q235 specimen after tensile testing. No delamination was observed on the bonding surface, and no cracks were found on the nickel foil surface, indicating good bonding quality at the interface. The fracture morphology of the composite plate interface was examined by SEM, and is shown in Figure 8. The tensile fracture shows obvious plastic deformation and dimpling, indicating ductile fracture characteristics on the fracture surfaces of both the Ni and steel sides, which is the reason for the high tensile strength of the composite plate under this condition. The high density of dimples in the fracture interface region may be attributed to the formation of a localized melting zone at the bond interface and process hardening caused by the blast impact. The localized high temperature and rapid cooling process that occurred at the bond surface after the high-speed collision of the metal materials partially restored the material toughness.

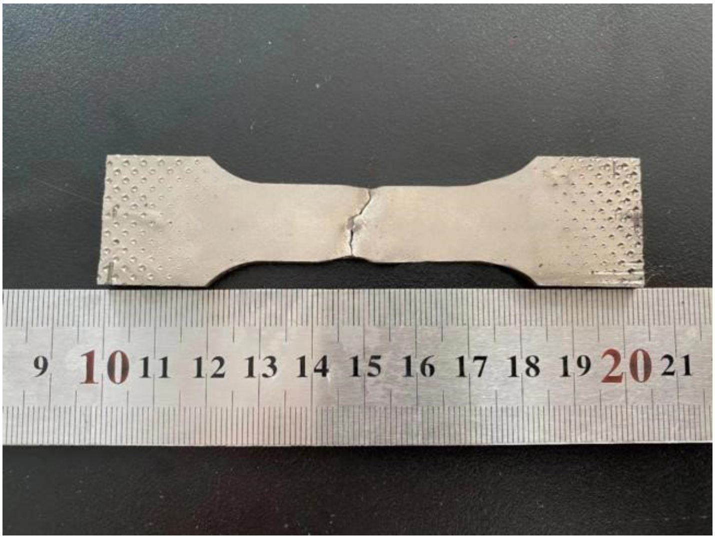

Figure 7. Specimen after stretching

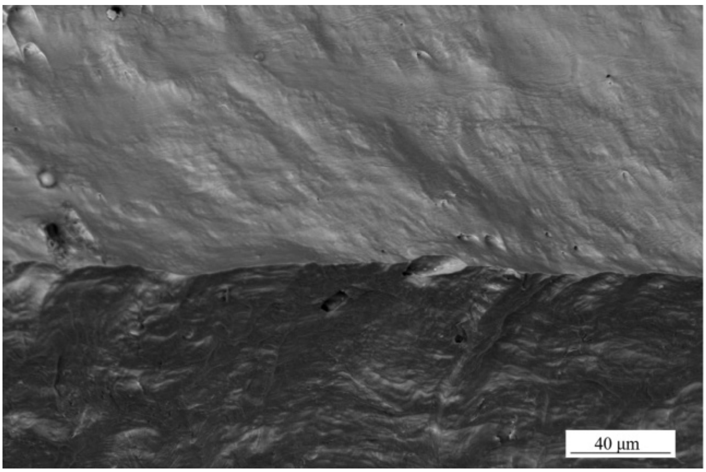

(a)

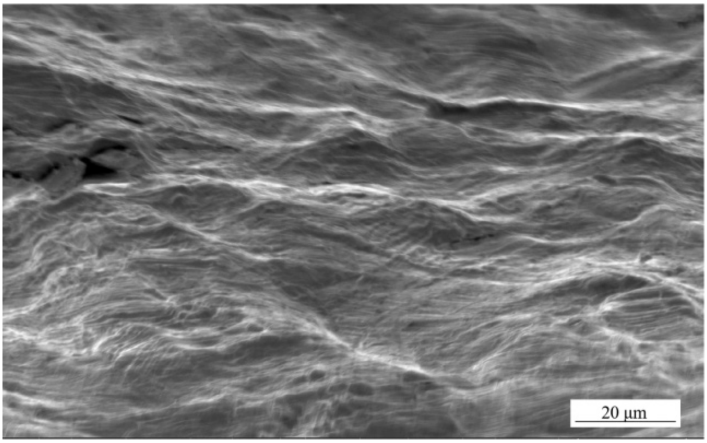

(b)

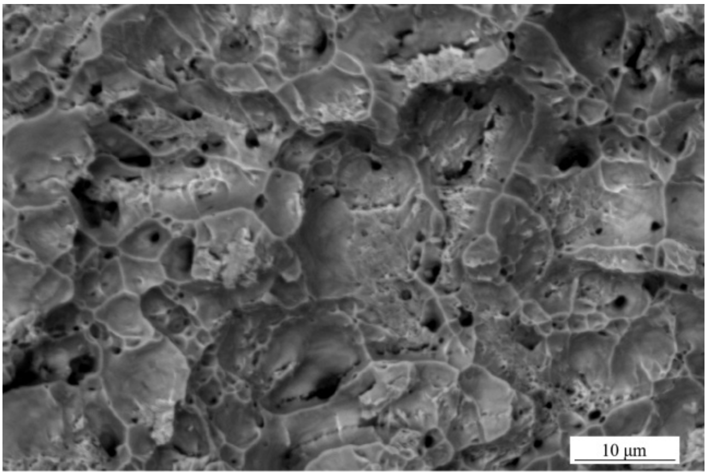

(c)

Figure 8. SEM of: Ni/Q235 tensile fracture (a), Ni lateral fracture (b) and Q235 lateral fracture (c)

4 SPH Simulation

4.1 Test model and material parameters

In the explosive welding process, the base composite plate undergoes high-speed collision and plastic deformation of the metal [20, 21], and the time required is extremely short, typically tens of milliseconds. Observing the details of the process directly is difficult using existing technology. To study the evolution of the bonding interface during the welding process, a two-dimensional planar model was established in ANSYS/AUTODYN, and the SPH method was used to reproduce the formation of the jet and the waveform of the weld [22]; a schematic diagram of the numerical simulation of Ni/Q235 explosive welding is shown in Figure 9.

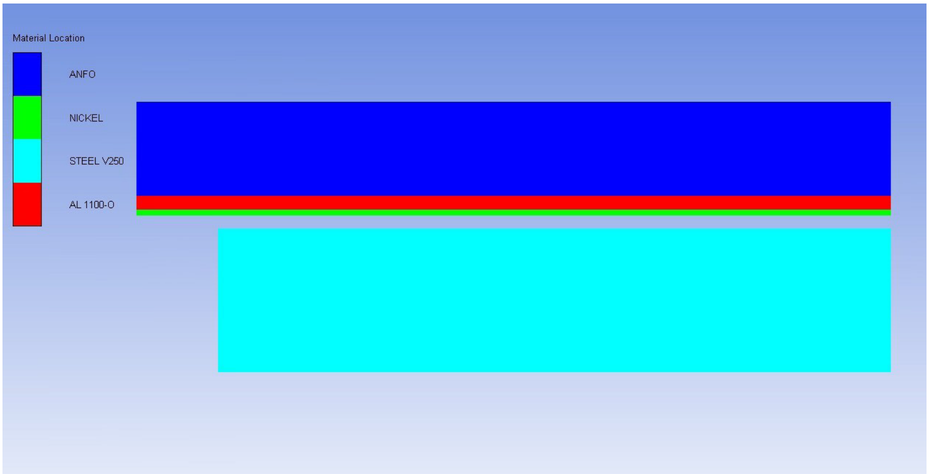

Figure 9. Schematic diagram of the numerical simulation model of explosive welding

In the collision process, the interface material experiences large deformation, high strain rate and high temperature and pressure, *etc*. The Mie-Grüneisen shock equation of state and the Steinberg-Guinan material model were used for the base complex plate.

The Mie-Grüneisen equation of state is used for the base complex plate material, and its equations are:

$$P = P_H + \Gamma_0 \rho_0 (e - e_H) \tag{2}$$

$$\Gamma_0 \rho_0 = \Gamma_p = Const \tag{3}$$

$$P_H = \frac{\rho_0 C_0^2 \mu (1+\mu)}{[1-(s-1)\mu]^2} \tag{4}$$

$$e_H = \frac{\rho_H}{2\rho_0}\left(\frac{\mu}{1+\mu}\right) \tag{5}$$

$$\mu = \frac{\rho}{\rho_0 - 1} \tag{6}$$

where Γ_0 is Grüneisen coefficient, P is pressure, P_H is pressure after material deformation, e is internal energy, C_0 is volumetric speed of sound, s is material parameter and μ is Poisson's ratio. The parameters of the equation of state are shown in Table 2.

Table 2. Material parameters of the Mie-Grüneisen shock equation

Materials	Γ_0	C_0 [km/s]	ρ_0 [g/cm^3]	s
Ni	1.930	4 650	8.900	1.445
Q235	1.600	3 980	7.850	1.580

For the choice of material model, the Steinberg-Guinan material model was used for all of the base complex plates [23].

$$\mu = \mu_0\left[1 + \mathrm{b}PV_1^{\frac{1}{3}} - \mathrm{h}(T_1 - 300)\right] \tag{7}$$

$$Y = \left[Y_0\left(1 + \beta_1 \bar{\varepsilon}^P\right)^n\right]\left[1 + bPV_1^{\frac{1}{3}} - h(T_1 - 300)\right] \tag{8}$$

$$Y_0[1 + \kappa\varepsilon]^n \leq Y_{max} \tag{9}$$

These formulas were used to calculate the shear modulus, where Y and Y_0 represent the current and initial yield pressures, ε is the effective plastic strain, V_1 is the relative volume, κ is the hardening constant, and n, b, h, and T_1 are given dielectric constants.

Table 3. Material parameters of the Steinberg-Guinan equation

Materials	μ_0 [GPa]	Y [GPa]	κ	n
Ni	85.5	0.14	46	0.53
Q235	71.8	1.56	2	0.50

4.2 Simulation results and interface morphology

In the numerical simulations of explosive welding, the jet phenomenon is often observed. Figure 4 shows the numerical simulation results of the Ni/Q235 explosive welding process, including the morphology of the composite plate waveform interface and the resulting jet, as shown in Figures 10 and 11.

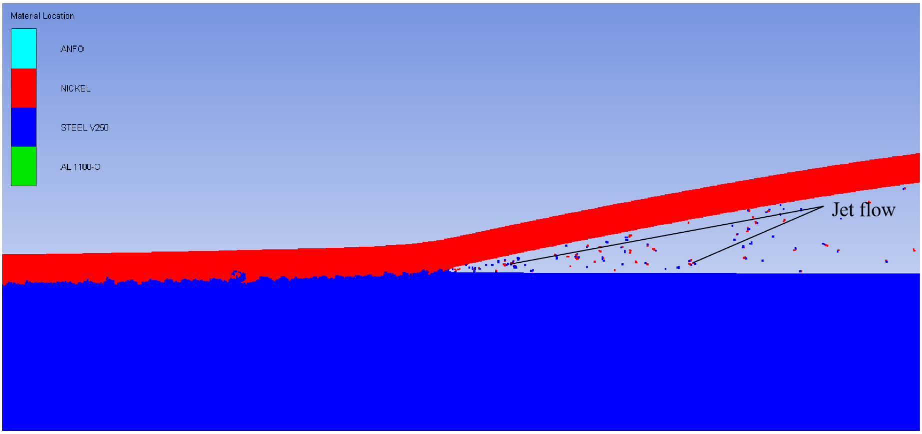

Figure 10. Numerical simulation process diagram of explosive welding

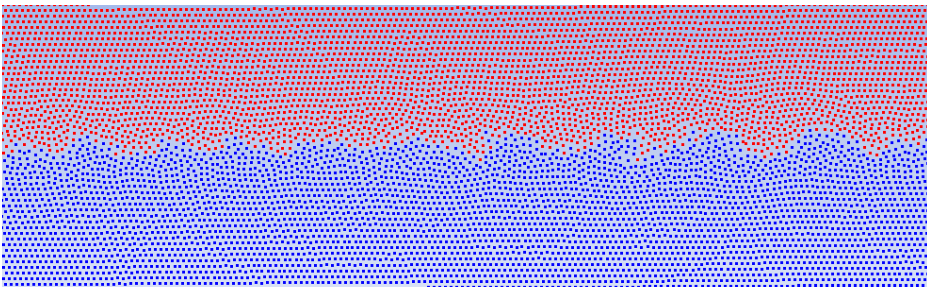

Figure 11. Schematic diagram of the numerical simulation interface of explosive welding

The numerical simulation process shown in Figures 10 and 11, combined with the interface morphology, reveals that the explosive welding process produces a significant jet and the formation of a waveform interface. Bataev *et al.* [23] have concluded that the presence of metal jets in the explosive welding process is a necessary condition for the formation of the waveform interface through SPH simulation. During the explosive welding process, one end of the explosive is initiated, and the explosion products form a high-pressure impact load that acts directly on the composite plate, accelerating it to several hundred meters per second in a very short period of time. The plates from the detonation of the explosive's starting section in turn collide with the substrate, and the two metal plates produce a great collision pressure during the collision process. This pressure greatly exceeds the dynamic yield limit of the metal (generally 10-12 times the dynamic yield limit), causing plastic deformation in the collision area. At this point, the metal plate's inner surface produces a metal jet that removes metal surface oxides and other impurities, exposing a clean surface, and ultimately improving the quality of the weld interface. A repeatedly disturbed jet will invade the substrate and compound plate, and eventually form a wavy interface. The numerical simulations show that the majority of the jet is provided by Q235, and less by the Ni foil, due to the fact that lower density materials are more likely to produce a jet during the explosive welding process [24]. The jet phenomenon and waveform morphology demonstrate that a good bond is achieved between the substrate and the composite plate.

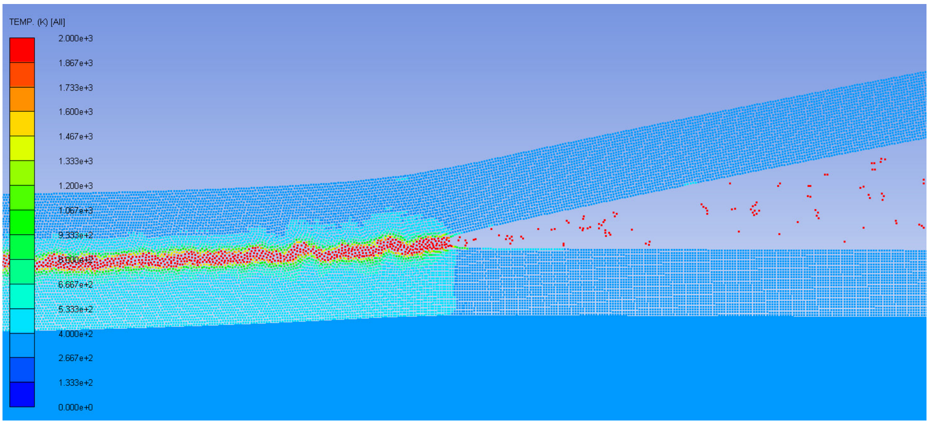

(a)

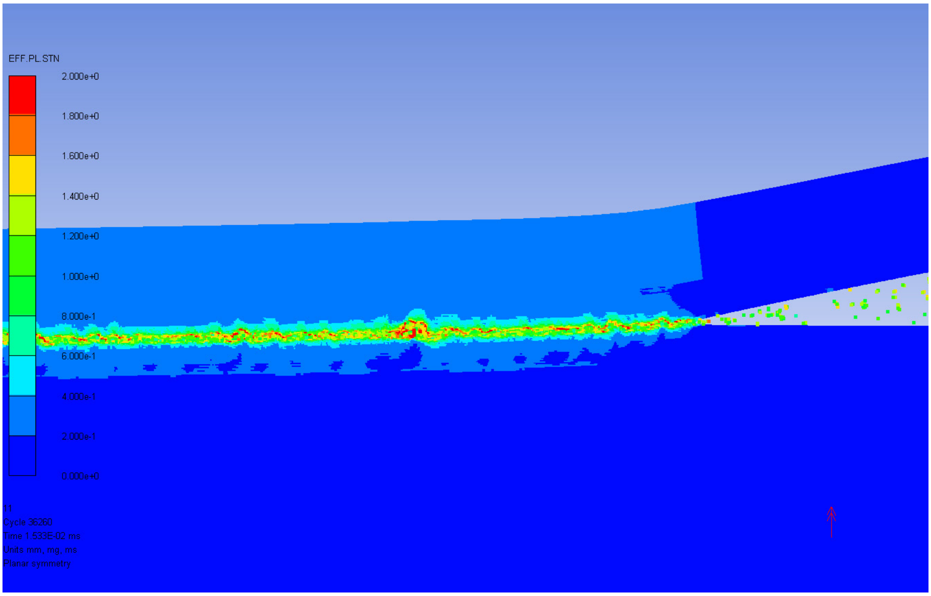

(b)

Figure 12. Temperature field (a) and shaping strain (b)

Figure 12(a) shows a numerical simulation of the temperature distribution during the explosive welding process. It is evident that the temperature at the interface can exceed 1800 K, which is higher than the melting point of Ni (1726 K) and Q235 steel (1766 K). This indicates the occurrence of local melting at the Ni/Q235 interface during the explosive welding process. Figure 12(b) presents the strain distribution at the composite plate interface during the numerical simulation. The collision pressure causes significant plastic deformation in the substrate and composite plate, resulting in a narrow plastic deformation zone at the interface bonding region.

Figure 13 displays the stress curves of the composite plate interface during the numerical simulation, where three pairs of measurement points are taken at the collision surfaces of the Ni foil and steel plate, respectively. The yield strengths of the Ni foil and steel plate are 100 and 235 MPa, respectively. The stress curves and stress distributions reveal that the composite plate interface is subjected to immense stress, with the pressure on the Ni side exceeding 30 GPa and the pressure on the steel side reaching 19 GPa, which are much higher than the yield strength of the materials. Therefore, the high pressure at the bond interface is the main reason for the formation of the waveform interface at the Ni/Q235 bond interface.

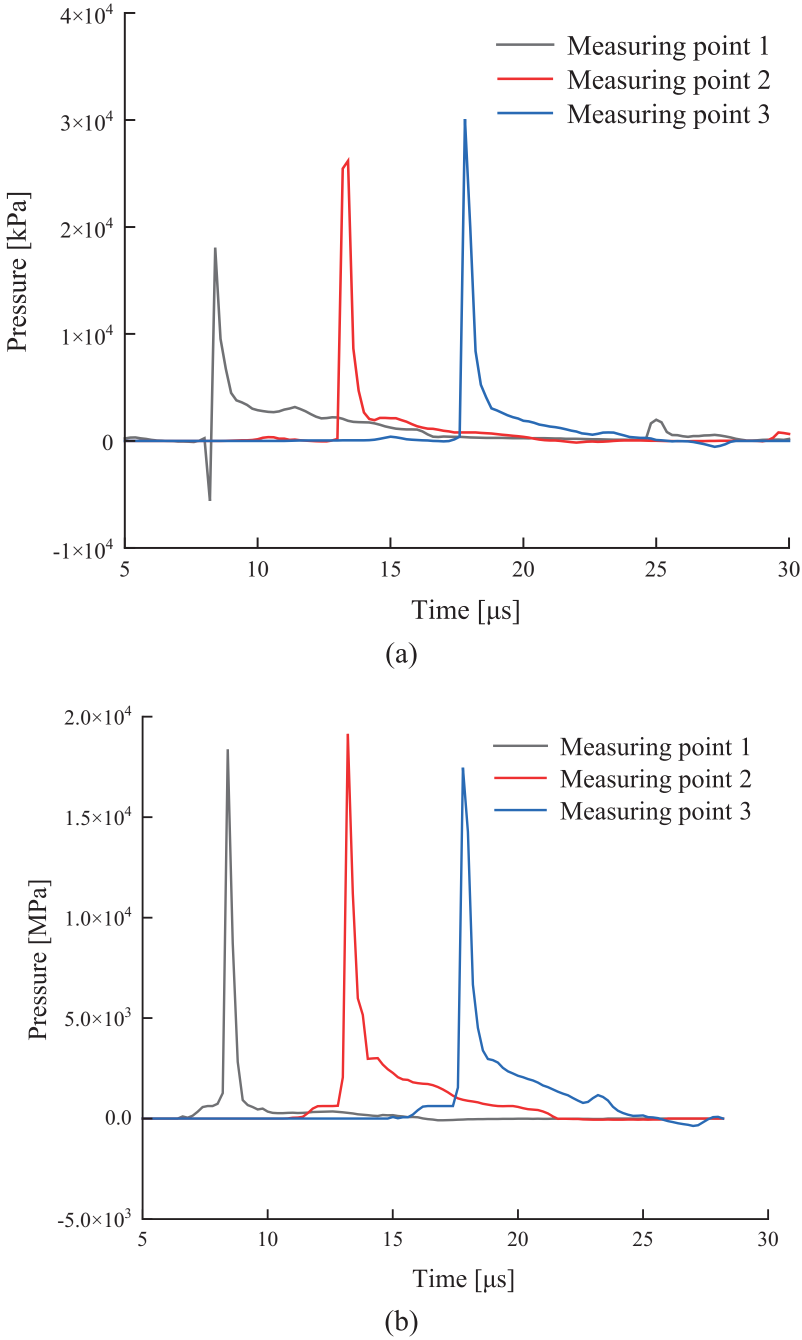

Figure 13. Lateral pressures for Ni (a) and Q235 (b)

5 Conclusions

- ♦ The composite plate obtained from Ni foil and Q235 steel, using explosive welding technology, has a regular waveform bonding interface, with a discontinuous melting layer and no observable cracks or holes.
- ♦ SEM and EDS tests indicated that the bonding interface has a clear waveform and some diffusion occurs, with a diffusion layer thickness of approximately 10 μm.
- ♦ The composite plate of Ni foil and Q235 steel exhibits no separation at the bonding interface during tensile testing, and its tensile strength is higher than that of the Q235 steel plate prior to the composite formation. The composite plate's tensile strength was 623 MPa, and ductile fracture occurs near the interface after tensile fracture.
- ♦ Numerical simulation results indicated that the explosive welding process produces a significant jet at the joint interface. The pressure distribution at the interface greatly exceeds the yield strength of the materials, which is the primary reason for the formation of the waveform interface.

References

[1] Borchers, C.; Lenz, M.; Deutges, M.; Klein, H.; Gärtner, F.; Hammerschmidt, M; Kreye, H. Microstructure and Mechanical Properties of Medium-Carbon Steel Bonded on Low-Carbon Steel by Explosive Welding. *Mater. Des.* **2016**, *89*(5): 369-376; https://doi.org/10.1016/j.matdes.2015.09.164.

[2] Kahraman, N.; Gülenç, B. Microstructural and Mechanical Properties of Cu-Ti Plates Bonded through Explosive Welding Process. *J. Mater. Process. Technol.* **2005**, *169*(1): 67-71; https://doi.org/10.1016/j.jmatprotec.2005.02.264.

[3] Akbari Mousavi, S.A.A.; Farhadi Sartangi, P.F. Experimental Investigation of Explosive Welding of cp-Titanium/AISI 304 Stainless Steel. *Mater. Des.* **2009**, *30*(3): 459-468; https://doi.org/10.1016/j.matdes.2008.06.016.

[4] Zheng, Y. Principle and Application of Explosive Welding and Explosive Composite Materials. *Welding Technology* **2007**, *36*(4); ISBN 9787811055092.

[5] Findik, F. Recent Developments in Explosive Welding. *Mater. Des.* **2011**, *32*(3): 1081-1093; https://doi.org/10.1016/j.matdes.2010.10.017.

[6] Durrani, T. A Study of Electroless Nickel-Boron Coating Process. *J. Chem. Soc. Pak.* **2011**, *30*(6): 536.

[7] Legkaya, D.A.; Solov'eva, N.D.; Yakovlev, A.V. Physicomechanical Properties of Nickel Coating Deposited from Sulfate Nickel Plating Electrolyte Using Preliminary Underpotential Deposition. *Russ. J. Appl. Chem.* **2017**, *90*(9): 1454-1458; https://doi.org/10.1134/S1070427217090129.

[8] Lysak, V.I.; Kuzmin, S.V. Energy Balance During Explosive Welding. *J. Mater. Process. Technol*. **2015**, *222*: 356-364; https://doi.org/10.1016/j.jmatprotec.2015.03.024.
[9] Hokamoto, K.; Nakata, K.; Mori, A.; Tsuda, S.; Tsumura, T.; Inoue, A. Dissimilar Material Welding of Rapidly Solidified Foil and Stainless Steel Plate Using Underwater Explosive Welding Technique. *J. Alloys Compd*. **2009**, *472*(1-2): 507-511; https://doi.org/10.1016/j.jallcom.2008.05.002.
[10] Zhou, Q.; Feng, J.; Chen, P. Numerical and Experimental Studies on the Explosive Welding of Tungsten Foil to Copper. *Materials* **2017**, *10*(9): 984; https://doi.org/10.3390/ma10090984.
[11] Liu, W.D.; Liu, K.X.; Chen, Q.Y.; Wang, J.T.; Li, X.J. Metallic Glass Coating on Metals Plate by Adjusted Explosive Welding Technique. *Appl. Surf. Sci*. **2009**, *255*(23): 9343-9347; https://doi.org/10.1016/j.apsusc.2009.07.033.
[12] Yang, M.; Ma, H.; Shen, Z.; Huang, Z.; Tian, Q.; Tian, J. Dissimilar Material Welding of Tantalum Foil and Q235 Steel Plate Using Improved Explosive Welding Technique. *Mater. Des.* **2020**, *186*: paper 108348; https://doi.org/10.1016/j.matdes.2019.108348.
[13] Wang, X.; Zheng, Y.; Liu, H. Numerical Study of the Mechanism of Explosive/Impact Welding Using Smoothed Particle Hydrodynamics Method. *Mater. Des.* **2012**, *35*: 210-219; https://doi.org/10.1016/j.matdes.2011.09.047.
[14] Miao, G.; Ma, H.; Shen, Z. Honeycomb Structural Explosive and Its Application. *J. Energ. Mater.* **2014**, *22*(5): 693-697.
[15] Bahadur Sherpa, B.; Dinesh Kumar, P.; Upadhyay, A.; Kumar, S.; Agarwal, A.; Tyagi, S. Low Velocity of Detonation Explosive Welding (LVEW) Process for Metal Joining. *Propellants Explos. Pyrotech*. **2020**, *45*(10): 1554-1565; https://doi.org/10.1002/prep.202000019.
[16] Hoseini Athar, M.M.; Tolaminejad, B. Weldability Window and the Effect of Interface Morphology on the Properties of Al/Cu/Al Laminated Composites Fabricated by Explosive Welding. *Mater. Des.* **2015**, *86*: 516-525; https://doi.org/10.1016/j.matdes.2015.07.114.
[17] Zhao, H. Characterization of the Microstructure and Bonding Properties of Zirconium-Carbon Steel Clad Materials by Explosive Welding. *Scanning* **2020**, *2020*: paper 8881898; https://doi.org/10.1155/2020/8881898.
[18] Wang, S.; Han, X. Investigation on Microstructure and Mechanical Properties of TA10-Q245R Composite Plate Formed by Explosive Welding. *J. Mater. Eng. Perform.* **2019**, *28*(7): 4241-4251; https://doi.org/10.1007/s11665-019-04193-x.
[19] National standard GB/T228-200 *Room Temperature Tensile Test Method for Metal Materials.* (in Chinese) China.
[20] Liu, L.; Jia, Y.-F.; Xuan, F.-Z. Gradient Effect in the Waved Interfacial Layer of 304L/533B Bimetallic Plates Induced by Explosive Welding. *Mater. Sci. Eng. A* **2017**, *704*: 493-502; https://doi.org/10.1016/j.msea.2017.08.012.
[21] Zhang, Z.L.; Liu, M.B. Numerical Studies on Explosive Welding with ANFO by

Using a Density Adaptive SPH Method. *J. Manuf. Process.* **2019**, *41*: 208-220; https://doi.org/10.1016/j.jmapro.2019.03.039.
[22] Peng, J.; Hu, C.; Li, Y.; Zhang, L.; Jing, F. Determination of Parameters of Steinberg-Guinan Constitutive Model with Shock Wave Experiments. *Int. J. Mod. Phys. B* **2008**, *22*(09n11): 1111-1116; https://doi.org/10.1142/S0217979208046396.
[23] Bataev, I.A.; Tanaka, S.; Zhou, Q.; Lazurenko, D.V.; Jorge Junior, A.M.; Bataev, A.A.; Hokamoto, K.; Mori, A.; Chen, P. Towards Better Understanding of Explosive Welding by Combination of Numerical Simulation and Experimental Study. *Mater. Des.* **2019**, *169*: 107649; https://doi.org/10.1016/j.matdes.2019.107649.
[24] Yuan, X.; Wang, W.; Cao, X.; Zhang, T.; Xie, R.; Liu, R. Numerical Study on the Interfacial Behavior of Mg/Al Plate in Explosive/Impact Welding. *Sci. Eng. Compos. Mater*. **2017**, *24*(4): 581-590; https://doi.org/10.1515/secm-2015-0316.

Received: February 26, 2023
Revised: September 25, 2023
First published online: September 28, 2023